Nonlinear dynamics of a microelectromechanical oscillator with delayed feedback

R. van Leeuwen,[1,*] D. M. Karabacak,[2] H. S. J. van der Zant,[1] and W. J. Venstra[1,†]

[1]*Kavli Institute of Nanoscience, Delft University of Technology, Lorentzweg 1, 2628 CJ Delft, The Netherlands*

[2]*Holst Centre/imec The Netherlands, High Tech Campus 31, 5656 AE Eindhoven, The Netherlands*

(Received 26 July 2013; revised manuscript received 25 October 2013; published 5 December 2013)

We study the dynamics of a nonlinear electromechanical oscillator with delayed feedback. Compared to their linear counterparts, we find that the dynamics is dramatically different. The well-known Barkhausen stability criterion ceases to exist, and two modes of operation emerge: one characterized by hysteresis in combination with a bistable frequency and amplitude; the other, by self-stabilization of the oscillation frequency and amplitude. The observed features are captured by a model based on a Duffing equation with delayed force feedback. Nonlinear oscillators with delayed force feedback are exemplary for a large class of dynamic systems.

DOI: 10.1103/PhysRevB.88.214301 PACS number(s): 85.85.+j, 05.45.−a

Oscillators are ubiquitous in nature and engineering, with implementations in physical, life, and social sciences.[1–3] Typical components of an oscillator are a resonant system and a positive feedback loop. Oscillators are self-sustained and produce an ac output signal from a dc input. Compared to a resonator, which is driven by an ac signal, an oscillator exhibits a reduced line width and improved phase-noise performance. These properties make them interesting as sensitive detectors and as timing references. A common example is the quartz crystal oscillator, with widespread application in electronic circuits.

In current applications the oscillating element is typically linear, implying that the displacement is proportional to the driving force as in Hooke's law. In a linear system, displacement-proportional feedback modifies the spring constant, whereas velocity-proportional feedback modifies the damping. Stability for the latter systems is bounded by the well-known Barkhausen criterion.[4,5] It states that a self-sustained oscillation occurs when the phase shift around the loop is an integer multiple of 2π, and the loop gain exceeds the value k/Q, where k is the spring constant and Q the quality factor without feedback. Although the linear regime has been studied in great detail, much less is known about nonlinear oscillating elements. In a nonlinear oscillator, the oscillating frequency depends on the amplitude of the motion. Micro- and nanoscale electromechanical devices exhibit strong nonlinearity, which makes them ideal devices to study such systems.[6–8] We demonstrate that in the presence of a delayed force feedback, the nonlinearity gives rise to intricate dynamic behavior near the oscillation threshold.

To construct a strongly nonlinear oscillator, we use a doubly clamped micromechanical beam with a high aspect ratio as the oscillating element. Figure 1(a) shows the device, with dimensions $L \times w \times h = 750 \times 8 \times 0.5\ \mu\text{m}^3$, fabricated from silicon nitride using standard microfabrication processes.[9] An integrated piezoelectric actuator enables periodic driving of the beam, as well as static tuning of its resonance frequency. The motion of the beam is probed with $\text{pm}/\sqrt{\text{Hz}}$ sensitivity using an optical deflection technique, by, is shown in Fig. 1(b), reflecting a laser beam off the surface of the device onto a position-sensitive photodetector.[10] The experiments are conducted at room temperature and atmospheric pressure. We start with open-loop measurements to characterize the dynamic properties of the oscillating element.

Figure 1(c) shows the response (magnitude and phase) at the fundamental resonance frequency, while driving the actuator with a sinusoidal voltage at three amplitudes V_d. When weakly driven, $V_d = 1$ V, the response resembles a harmonic resonator with a resonance frequency $f_0 = 125.9$ kHz, and a quality factor $Q_0 = 34$, typical for micromechanical resonators vibrating at atmospheric pressure. When driven more strongly, the resonance frequency depends on the driving voltage and the response line becomes asymmetric. The susceptibility[11] on resonance is constant, $|H| = 6.2$ mV/V, which indicates that the vibration amplitude is proportional to the driving force, and nonlinear damping plays no significant role in these experiments.[12,13] In doubly clamped resonators, the nonlinearity stems from the displacement-induced tension, which becomes important when the vibration amplitude becomes comparable to the device thickness. Corrections to the spring constant should then be taken into account, which give rise to a stiffening of the resonator and a higher resonance frequency and bistability when driven beyond the critical amplitude.[14,15] Throughout this work, the resonator is driven below this amplitude, and although the nonlinearity is clearly present, the open-loop amplitude and phase response remain single-valued functions of the driving force.

To implement an oscillator we devise the feedback loop displayed in Fig. 2(a). The resonator is now driven only by its own motion, as the photodiode signal is amplified and fed back to the piezo actuator. The feedback signal is delayed by $\tau = 5.9\ \mu$s, which gives rise to a phase lag $\phi = 1.49\pi \approx \frac{3}{2}\pi$ between the driving signal and the beam displacement. Thus, the feedback force is closely proportional to the velocity of the resonator and compensates the viscous damping force. This behavior is verified by measuring the power spectral density (PSD) of the displacement noise in Fig. 2(b). Without amplification ($G = 0$) the oscillation peak is not detected. Increasing the gain reduces the damping, and the oscillation peak emerges. The peak becomes narrower when the gain is increased, as the effective Q factor of the closed-loop system is given by $Q_{\text{eff}} = Q/(1 - G \cdot |H|)$. For $G > 161$ we observe an increase in the amplitude, which confirms the onset of self-sustained oscillations at $G \cdot |H| = 1$. Further increasing the gain results in a limit cycle at an amplitude dictated by the saturation value of the feedback amplifier. Interestingly, a frequency shift $\Delta f \approx 2$ kHz is observed upon entering the

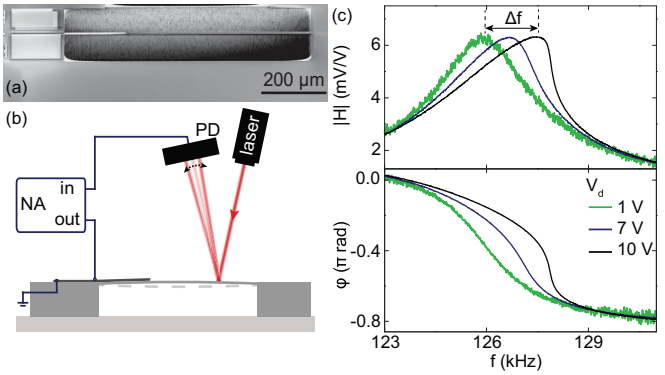

FIG. 1. (Color online) (a) Scanning electron microscope image of the silicon nitride beam with embedded piezoelectric actuator. (b) Schematic of the experimental setup. PD, two-segment position-sensitive photodetector; NA, network analyzer. (c) Open-loop network analyzer measurements (magnitude and phase response) of the resonator susceptibility at weak and strong driving.

regime of self-sustained oscillations, which is large compared to the oscillator line width and comparable to the frequency shift due to the Duffing nonlinearity shown in Fig. 1(b). As the time delay in the feedback loop is fixed, this change in the oscillation frequency significantly alters the effective feedback force, which gives rise to intriguing dynamics near the threshold of self-sustained oscillations.

To study this behavior in more detail, we adjust the phase between the feedback signal and the beam motion by tuning the eigenfrequency of the beam via the residual stress. Applying a dc voltage to the piezo tunes the mode by 200 Hz/V,[16] and this provides a means to accurately modify the phase over a few tens of milliradians around $\phi_0 = \frac{3}{2}\pi$. In the following discussion, f_0 denotes the tuned open-loop eigenfrequency of the oscillating element; $f_{\rm osc}$, the peak frequency of the

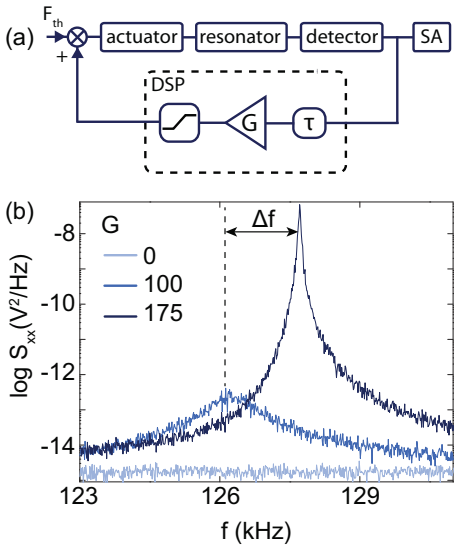

FIG. 2. (Color online) (a) Schematic of the feedback loop. The delay time (τ), feedback gain (G), and limiter are implemented in a digital signal processor. SA, spectrum analyzer. (b) Closed-loop measurement of the displacement noise power spectral density at the indicated feedback gain.

closed-loop system; and $\Delta f = f_{\rm osc} - f_0$, the frequency shift in the closed loop. $\delta = \phi - \phi_0$ denotes the offset of the phase of the feedback signal from the velocity-proportional condition.

Close to the oscillation threshold we fine-tune the parameter δ and measure the displacement-noise power spectral density of the oscillator to determine the frequency shift Δf for different values of G. Figure 3(a) shows the results. For $\delta > 0$ (top panel) a continuous and monotone increase in the oscillation frequency and amplitude is observed. There is no clear oscillation threshold, as the frequency and amplitude continuously increase towards the saturated value. The traces for increasing and decreasing G coincide. In contrast, for $\delta < 0$, a clear oscillation threshold exists, marked by a transition of Δf. Both the oscillator amplitude and its frequency are discontinuous functions of the gain. Moreover, the oscillation frequency shows hysteresis as the gain is swept forward and backward. A regime of bistability exists, where the oscillation threshold for an upwards sweep occurs at a higher gain than in the reverse direction.

We have performed a systematic study of the oscillation threshold by fine-tuning the eigenfrequency of the beam over range of positive and negative δ. A two-dimensional map is constructed by sweeping the gain from a low to a high value, and vice versa, for a range of eigenfrequencies f_0, which corresponds to a phase adjustment over several tens of milliradians around $\frac{3}{2}\pi$. Figure 3(b) shows the oscillator frequency for a range of G and f_0, where each pixel represents a frequency shift Δf as determined from a noise spectrum [cf. Fig. 2(b)]. The gain is swept from a low to a high value in the upper panel, and the reverse occurs in the lower panel. The regimes are characterized by a continuous increase in the oscillator amplitude and frequency for $\delta > 0$ and bistable hysteretic transitions for $\delta < 0$. The condition $\delta = 0$, indicated by the dotted horizontal white line in the figure, separates the two regimes. The width of the hysteresis is indicated by the dashed black line in the lower panel.

Intuitively, the observations are explained as follows. When the amplitude of the motion increases, the nonlinearity shifts the oscillation frequency to a higher value and this reduces the delay time required to match the oscillation condition. This mechanism presents a feedback loop in itself and gives rise to either an escalation or a stabilization of the motion in the vicinity of the critical point. In the case where $\delta > 0$, the oscillator phase increases by the nonlinear frequency shift, which causes the system to move away from the oscillation condition. Here, the nonlinear frequency pulling stabilizes the oscillation amplitude and frequency. The oscillation threshold vanishes, as the frequency and amplitude increase continuously with the gain. When $\delta < 0$ an upwards frequency shift pushes the system farther into the instable regime. The system collapses, which gives rise to a distinct oscillation threshold, beyond which a transition in the frequency and the amplitude of the oscillation occurs. When the gain is swept in the reverse direction, a different branch is followed as, at a higher frequency, the oscillation can remain self-sustained at a lower gain.

To perform a more quantitative analysis of the experiment, we calculate the dynamic behavior. The system in its simplest form is modeled by a nonlinear Duffing oscillator with a

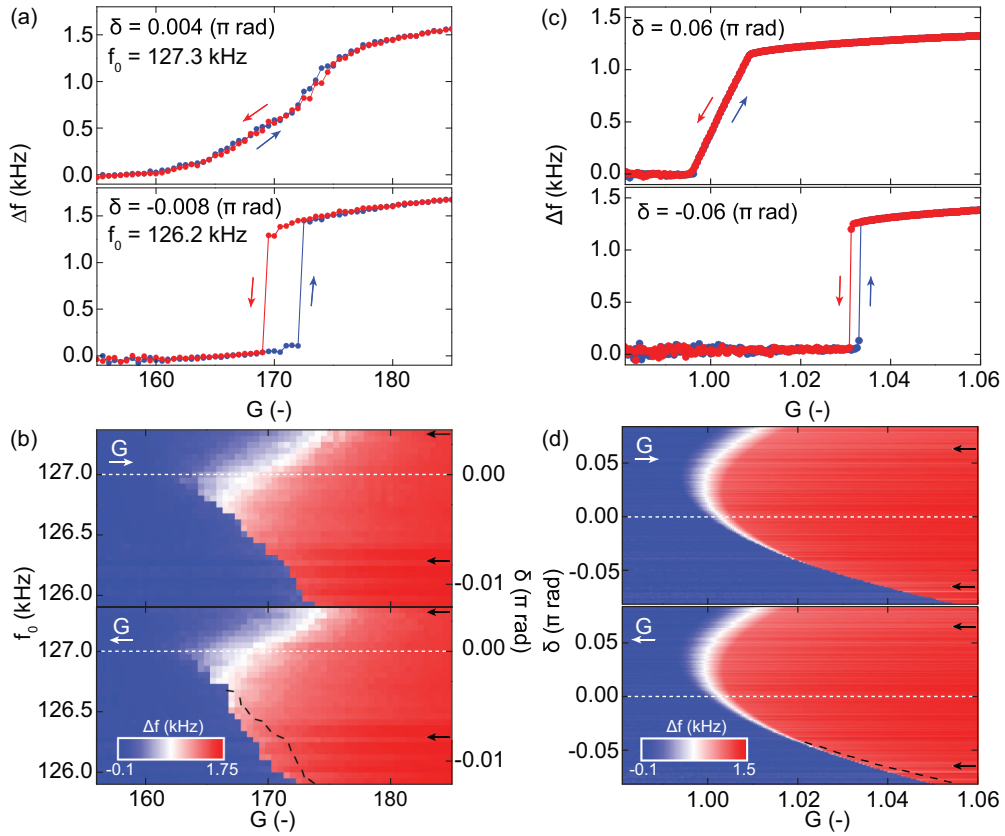

FIG. 3. (Color online) (a) Oscillation frequency for different values of G, for $f_0 = 126.2$ kHz and $f_0 = 127.3$ kHz. The arrow indicates the sweep direction. (b) Full measurement from which the cross sections (a) are taken. The color scale indicates Δf, as obtained from the noise spectrum. f_0 is swept by applying a constant voltage to the piezo actuator. (c), (d) Calculated oscillator frequency with parameters similar to those in the experiment. The dashed black line in (b) and (d) indicates the region of hysteresis.

time-delayed force feedback and amplitude saturation as follows:

$$m\ddot{x} + \frac{m(2\pi f_0)}{Q_0}\dot{x} + m(2\pi f_0)^2 x + \alpha x^3 = Ghx(t-\tau) + F_{\text{th}},$$
$$|Gx(t-\tau)| < L. \qquad (1)$$

Here, m is the total mass of the resonator, x is the resonator displacement, f_0 is the linear resonance frequency, Q_0 is the open-loop quality factor, G is the total feedback gain, and τ is the delay time. h is the transduction gain, which depends on the laser power and the alignment of the optics. The parameter α represents the strength of the nonlinear restoring force. An over dot denotes taking the derivative to time. The system is driven by a stochastic force F_{th}, and the feedback force is limited by L. We calculate the frequency shifts with parameters similar to the values in the experiment, $m = 7.8 \times 10^{-12}$ kg, $Q_0 = 34$, and $\alpha = 2.6 \times 10^{21}$ kg/m^2 s^2, as estimated from the device geometry.[17] The delay time is $\tau = 5.9$ μs, which yields a $\frac{3}{2}\pi$ phase shift at $f_0 = 127$ kHz. With these parameters, Eq. (1) is integrated using a fourth-order Runge-Kutta method, and the frequency shift Δf is determined by taking the fast Fourier transform of the calculated time series in the steady state. Figure 3(c) shows the frequency shifts for positive and negative detuning. As in the experiment, for $\delta > 0$ (top panel) a continuous and monotone gain dependence is the result, while an hysteretic transition characterizes the regime with $\delta < 0$. For the parameters corresponding to the experiment, the frequency shifts are presented in Fig. 3(d). The simulation results confirm the emergence of the two regimes, the hysteresis, and the minimum gain to reach the oscillation threshold at $\phi = \frac{3}{2}\pi$.

The bistability for $\delta < 0$ enables the oscillator to function as a mechanical switch. In contrast to mechanical switches based on Duffing *resonators*,[18–20] the *oscillator*-based switch presented here is driven by a dc source. Moreover, as shown in Fig. 1(b), the strength of the driving force in the oscillator switch is below the critical amplitude for open-loop bistability, which enables the switch to function at a lower power. This is possible, as in a nonlinear oscillator the bistability is due to a change in the efficiency of the feedback force caused by nonlinearity. This gives rise to a Hopf-type bifurcation,[21] which should be contrasted to the saddle-node bifurcation that characterizes a Duffing resonator.

To demonstrate the micromechanical oscillator switch, we prepare the oscillator in a bistable state, and control its state by adjusting the loop gain.[22] Figure 4(a) shows the noise spectra of the oscillator-based switch; the insets represent its state schematically. For $\delta = -28$ mrad and $G = 102$ the oscillator is monostable in the low-amplitude and -frequency state, called the "low" state henceforward. For $G = 106$ the oscillator is monostable in the "high" state. For $G = 104$ the oscillator is bistable, and the "set" and "reset" operations are implemented by adjusting G as indicated in the inset in the middle panel. Since in the nonlinear oscillator both the

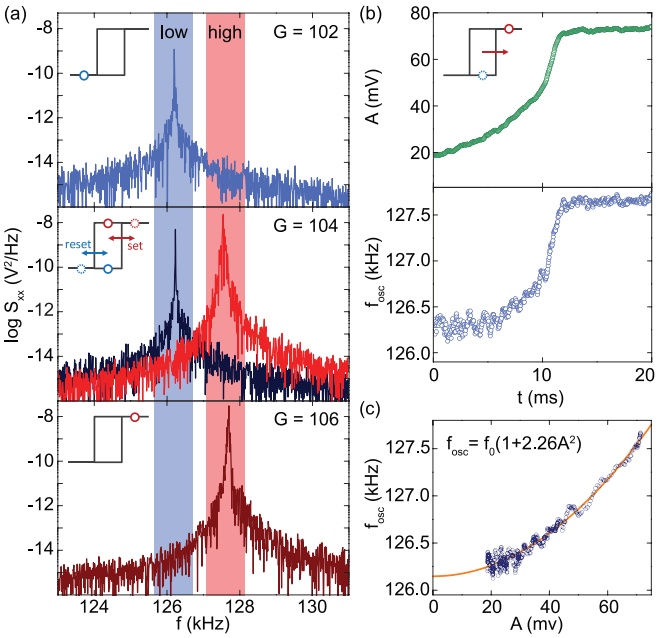

FIG. 4. (Color online) Switching and transient response in a bistable oscillator. (a) Monostability for $G = 102$ (top) and $G = 106$ (bottom). Bistability for $G = 104$ (middle). Insets: State of the oscillator and procedures to "set" and "reset" the switch. (b) Temporary amplitude (top) and frequency (bottom) during a switch from a "low" to a "high" state. (c) Relation between amplitude and frequency during the transient. Solid (red) line: quadratic fit.

amplitude and the frequency are bistable, during a switch both the oscillation amplitude and the frequency exhibit transient behavior. These are investigated now in more detail by a time-domain analysis of the oscillator amplitude and frequency during a transition. To record transitions, the gain is swept across the bistable regime while recording the photodiode signal using an oscilloscope. The instantaneous frequency and amplitude are then computed by fitting a piecewise sinusoidal function through the time series.

Figure 4(b) shows the oscillator amplitude and frequency during the transition from a low to a high state. Both the amplitude and the frequency of the oscillation depend on time, where the relaxation time for the ring-up equals $\tau = 3.9$ ms. In Duffing resonators driven below the critical amplitude, the resonance frequency increases quadratically with the amplitude of the vibration. It is interesting to investigate whether this coupling also is present in a Duffing oscillator, during a transition between two oscillating states. Figure 4(c) shows the frequency as a function of the oscillation amplitude: indeed a quadratic coupling is observed in the transients, with $\frac{\Delta f}{f_0} = 2.26A^2$. A calculation using Eq. (1) confirms the quadratic coupling between the transient responses. Thus, the observed transients in the bistable oscillator are well described by the cubic nonlinearity.

Nonlinearity is an important theme in micro- and nanomechanical devices.[12,23] It may arise from intrinsic geometric origins, as in cantilevers and doubly clamped beams,[17,24,25] or from an externally applied nonlinear field such as the electrostatic force.[26] Depending on the origin of the nonlinearity, the nonlinear spring constant can be positive or negative. When an oscillator is constructed from such devices, the phenomena described in this paper can be observed, as the dynamics are described by Eq. (1). Considering that the nonlinearity parameter α can be positive or negative, the near-threshold behavior will be stabilizing when $\alpha \cdot \delta > 0$ and hysteretic when $\alpha \cdot \delta < 0$. In this realm new applications emerge, such as mechanical switches and variable-frequency generators, driven by a dc source. In the stabilizing regime, i.e., on the steep slope in Figs. 3(a) and 3(c), the nonlinearity amplifies changes in the eigenfrequency. This principle may be used to enhance the response of oscillator-based sensors.

In conclusion, we have investigated the dynamics of a nonlinear microelectromechanical oscillator with delayed force feedback. The near-threshold behavior strongly deviates from that of a linear oscillator, as distinct regimes of stabilization and hysteresis emerge. Both the steady-state and the transient dynamics are captured by a simple model based on a Duffing equation with delayed feedback. Although the characteristic dynamics described in this paper are particularly relevant to micro- and nanomechanical systems, the behavior is by no means restricted to mechanical oscillators. Truly linear systems are rare in nature, and feedback with a fixed delay time occurs typically when a signal propagates from a sensing to an actuating device. We therefore anticipate that the presented analysis is applicable to a large class of dynamical systems.

The authors acknowledge financial support from NanoNextNL, a micro- and nanotechnology consortium of the Government of the Netherlands and 130 partners, and the European Union's Seventh Framework Programme (FP7) under Grant Agreement No. 318287, project LANDAUER.

*r.vanleeuwen-1@tudelft.nl
†w.j.venstra@tudelft.nl

[1] A. H. Nayfeh and D. T. Mook, *Nonlinear Oscillations* (Wiley, New York, 1995).
[2] C. T. C. Nguyen, IEEE Trans. Ultrason. Ferroel. Freq. Contr. **54**, 251 (2007).
[3] P. G. Steeneken, K. Le Phan, M. J. Goossens, G. E. J. Koops, G. J. A. M. Brom, C. van der Avoort, and J. T. M. van Beek, Nature Phys. **7**, 354 (2011).
[4] H. Barkhausen, *Lehrbuch der Elektronen-Röhren, 3. Band Rückkopplung* (Verlag von S. Hirzel, Leipzig, Germany, 1935).
[5] E. Lindberg, *18th IEEE Workshop of Nonlinear Dynamics of Electronic Systems (NDES2010)* (IEEE, Dresden, Germany, 2010).
[6] D. S. Greywall, B. Yurke, P. A. Busch, A. N. Pargellis, and R. L. Willett, Phys. Rev. Lett. **72**, 2992 (1994).
[7] L. Villanueva, R. Karabalin, M. Matheny, E. Kenig, M. Cross, and M. Roukes, Nano Lett. **11**, 5054 (2011).
[8] L. G. Villanueva, E. Kenig, R. B. Karabalin, M. H. Matheny, R. Lifshitz, M. C. Cross, and M. L. Roukes, Phys. Rev. Lett. **110**, 177208 (2013).
[9] D. M. Karabacak, S. H. Brongersma, and M. Crego-Calama, Lab Chip **10**, 1976 (2010).

[10]K. Babaei Gavan, E. W. J. M. van der Drift, W. J. Venstra, M. R. Zuiddam, and H. S. J. van der Zant, J. Micromech. Microeng. **19**, 035003 (2009).

[11]The susceptibility $|H|$ is defined as the rms amplitude of the amplified photodiode signal normalized to the voltage applied to the piezoelectric actuator.

[12]R. Lifshitz and M. C. Cross, *Reviews of Nonlinear Dynamics and Complexity* (Wiley, New York, 1998).

[13]A. Eichler, J. Moser, J. Chaste, M. Zdrojek, I. Wilson-Rae, and A. Bachtold, Nature Nanotechnol. **6**, 339 (2011).

[14]H. K. Lee, R. Melamud, S. Chandorkar, J. Salvia, S. Yoneoka, and T. W. Kenny, J. Microelectromech. Syst. **20**, 1228 (2011).

[15]R. M. C. Mestrom, R. H. B. Fey, and H. Nijmeijer, IEEE ASME Trans. Mechatron. **14**, 423 (2009).

[16]R. van Leeuwen, D. M. Karabacak, S. H. Brongersma, M. Crego-Calama, H. S. J. van der Zant, and W. J. Venstra, Microelectron. Eng. **98**, 463 (2012).

[17]H. W. C. Postma, I. Kozinsky, A. Husain, and M. L. Roukes, Appl. Phys. Lett. **86**, 223105 (2005).

[18]R. L. Badzey, G. Zolfagharkhani, A. Gaidarzhy, and P. Mohanty, Appl. Phys. Lett. **85**, 3587 (2004).

[19]J. S. Aldridge and A. N. Cleland, Phys. Rev. Lett. **94**, 156403 (2005).

[20]Q. P. Unterreithmeier, T. Faust, and J. P. Kotthaus, Phys. Rev. B **81**, 241405 (2010).

[21]S. H. Strogatz, *Nonlinear Dynamics and Chaos*, *Studies in Nonlinearity* (Perseus, Cambridge, MA, 2000).

[22]Due to the different alignment of the optical setup, the detector gain is lower compared to that in the previous experiment, and a slightly higher G is required to reach the oscillation threshold.

[23]K. L. Turner, S. A. Miller, P. G. Hartwell, N. C. MacDonald, S. H. Strogatz, and S. G. Adams, Nature **396**, 149 (1998).

[24]H. J. R. Westra, M. Poot, H. S. J. van der Zant, and W. J. Venstra, Phys. Rev. Lett. **105**, 117205 (2010).

[25]W. J. Venstra, H. J. R. Westra, and H. S. J. van der Zant, Appl. Phys. Lett. **97**, 193107 (2010).

[26]C. Lotze, M. Corso, K. J. Franke, F. von Oppen, and J. I. Pascual, Science **338**, 779 (2012).